Monthly Notices
of the
ROYAL ASTRONOMICAL SOCIETY

Mon. Not. R. Astron. Soc. **399,** 1964–1976 (2009) doi:10.1111/j.1365-2966.2009.15276.x

How selection and weighting of astrometric observations influence the impact probability. The case of asteroid (99942) Apophis

Małgorzata Królikowska,[1⋆] Grzegorz Sitarski[1] and Andrzej M. Sołtan[2]

[1]*Space Research Centre of the Polish Academy of Sciences, Bartycka 18A, 00-716 Warsaw, Poland*
[2]*Nicolaus Copernicus Astronomical Center, Bartycka 18, 00-716 Warsaw, Poland*

Accepted 2009 June 18. Received 2009 May 18; in original form 2009 January 22

ABSTRACT

The aim of this paper is to show that in the case of a low probability of asteroid collision with the Earth, the appropriate selection and weighting of the data are crucial for the impact investigation and for analysing the impact possibilities using extensive numerical simulations. By means of the Monte Carlo special method, a large number of 'clone' orbits have been generated. A full range of orbital elements in the six-dimensional parameter space, that is, in the entire confidence region allowed by the observational material, has been examined. On the basis of 1000 astrometric observations of (99942) Apophis, the best solutions for the geocentric encounter distance of $6.065 \pm 0.081\,R_\oplus$ (without perturbations by asteroids) or $6.064 \pm 0.095\,R_\oplus$ (including perturbations by the four largest asteroids) were derived for the close encounter with the Earth on 2029 April 13. The present uncertainties allow for special configurations ('keyholes') during this encounter that may lead to very close encounters in future approaches of Apophis. Two groups of keyholes are connected with the close encounter with the Earth in 2036 (within the minimal distance of $5.7736-5.7763\,R_\oplus$ on 2029 April 13) and 2037 (within the minimal distance of $6.3359–6.3488\,R_\oplus$). The nominal orbits for our most accurate models run almost exactly in the middle of these two impact keyhole groups. A very small keyhole for the impact in 2076 has been found between these groups at the minimal distance of $5.97347\,R_\oplus$. This keyhole is close to the nominal orbit. The present observations are not sufficiently accurate to eliminate definitely the possibility of impact with the Earth in 2036 and for many years after.

Key words: methods: data analysis – minor planets, asteroids – planets and satellites: individual: Apophis.

1 INTRODUCTION

The discovery of an asteroid that could possibly collide with the Earth in the foreseeable future is often a cause for concern in the astronomical community. Fortunately, so far this potential risk of collision has decreased as more observations have been collected. To date, the impact probability estimates of known potentially hazardous asteroids (at the beginning of 2009 there were more than 1000 such objects) are at most in the range of 10^{-4}–10^{-5}.[1] The main aim of this paper is to show that in the case of such low probabilities, the appropriate selection and weighing of the data are crucial for the impact investigation. To illustrate this, we have undertaken a very detailed analysis of the observational material and made extensive Monte Carlo analyses of the future encounters with the Earth of the asteroid (99942) Apophis.

This is a potentially dangerous object, as it is large (diameter 270 ± 60 m, Delbò, Cellino & Tedesco (2007)) and future collision possibilities have not yet been definitively solved. In addition, Apophis will not be observable until 2011 (Chesley 2006). The observational data collected in the months of 2004 March and 2006 August consist of 1000 optical and seven radar measurements. Here, we concentrate on the optical observations alone and show that the selection and weighting procedures applied to these observations provide the nominal orbit with an accuracy similar to that of the estimates found in the literature based on the astrometric and radar data.

We investigate the Apophis motion as a pure ballistic problem. Thus, we ignore non-gravitational (NG) effects. Obviously, to describe the asteroid orbit accurately, these effects should be included. The problem of NG effects is discussed by Giorgini et al. (2008). They show that the present data are insufficient to construct any

⋆E-mail: mkr@cbk.waw.pl

[1] At the time of writing, at the top of the list 'Objects Not Recently Observed' (Sentry Risk Table, NASA) are 2007 VK 184 with a cumulative probability of 3.4×10^{-4} and (99942) Apophis with a cumulative probability of 2.3×10^{-5}.

Table 1. Minimal distance in 2029 April for the various observational intervals. The weighting procedure was applied for each case independently.

Solution	Observational interval	Number of obs.	Number of residuals	rms (arcsec)	Minimal distance on 2029 April 13 [$R_\oplus$]
arc1	2004 06 19 – 2004 12 27	264	520	0.339	48.56 ± 6.98
arc2	2004 03 15 – 2004 12 27	270	535	0.352	5.542 ± 0.475
arc3	2004 03 15 – 2005 03 26	892	1771	0.316	6.699 ± 0.267
arc5	2004 03 15 – 2006 06 02	994	1965	0.316	6.564 ± 0.156
E	2004 03 15 – 2006 08 16	1000	1971	0.308	6.065 ± 0.081
arc6	2004 12 18 – 2006 08 16	988	1965	0.314	6.144 ± 0.078

reliable model of these effects. Thus, we are unable to predict precisely the Apophis trajectory in the distant future. The purely gravitational computations have been performed to show the potential Apophis behaviour, especially the keyhole ranges in 2036 and 2037 resulting from our full six-dimensional Monte Carlo method.

Some details of the Apophis story are worthy of note. The asteroid was discovered by Tucker, Tholen and Bernardi at Kitt Peak (Arizona) on 2004 June 19. Unfortunately, the object was lost until December 18, when it was rediscovered by Garradd from Siding Spring in Australia. On the basis of six months of observations, Apophis was recognized as a potentially hazardous asteroid with non-zero impact probability in 2029. However, substantial astrometric errors in the original June observations were quickly revealed (Chesley 2006). After remeasurements performed by Tholen, the impact probability was assessed at about 0.6 per cent, and during the following days this was systematically increased, reaching a peak of 2.7 per cent at the end of December. The pre-discovery observations from 2004 March, reported by the Spacewatch survey at the end of December, eliminated any possibility of an impact in 2029. Calculations based on observations from March to December have shown that the asteroid will pass near Earth on 2029 April 13 at a minimum distance of $10.1 \pm 2.6\,R_\oplus$ from the geocentre ($R_\oplus = 6378$ km). Moreover, it emerged that this deep encounter with Earth in 2029 implies resonant return encounters in subsequent years that could lead to several possible impacts.

Later, the radar astrometry obtained in late 2005 January from the Arecibo Observatory was reported to be inconsistent with this prediction (Smalley et al. 2005). Giorgini et al. (2005) found that radar data indicated a significantly closer approach of $5.6 \pm 1.6\,R_\oplus$. According to Chesley (2006), the discrepancy was explained by the systematic errors in the five pre-discovery observations of 2004 March, and remeasurements of these observations were undertaken by the Spacewatch team and T. Spahr from the MPC staff. The exciting story about changing the collision scenario of Apophis during December 2004 and January 2005 is described in detail by Sansaturio & Arratia (2008).

According to Giorgini et al. (2008), the new Arecibo radar observations of Apophis in 2005 August and 2006 May increased the close-approach distance on 2029 April 13 to $5.86 \pm 0.11\,R_\oplus$ and $5.96 \pm 0.09\,R_\oplus$, respectively ($38\,000 \pm 580$ km; closer than some geosynchronous communication satellites).

Table 1 summarizes the various calculations of the approach of Apophis to the Earth on 2029 April 13. We give the minimal distance from the Earth derived by us for the six different observational arcs based solely on the optical observations. It is worthwhile to note that the results based on 'arc6', which use neither the recalculated a posteriori observations of 2004 March and June nor the radar measurements, are similar to the results derived by Giorgini et al. (2008) on the basis of all the astrometric and radar data.

Although the risk of a collision with the Earth or the Moon in 2029 has been eliminated, there remains a very small possibility that, during the close encounter with Earth on 2029 April 13, Apophis will pass through a 'gravitational keyhole', a precise region in space that would set up a future impact on 2036 April 13.[2] In the present investigation we define the size of a keyhole by the distance range from the Earth's geocentre at the moment of close encounter on 2029 April 13. Our numerical calculations show that although the keyhole in 2029 for the 2036 impact is a 4–6 km wide, the impact risk is still extremely low.

In this paper we present details of the selection and weighting of Apophis observations and their effect on the best estimates of its position during the close safe encounter with Earth in 2029 and the possibility of impacts in 2036 and 2037. We are able to determine directly the sample of impact orbits for each close encounter with the Earth.

According to our impact calculations (Section 4), Apophis will hit Earth in 2036 only if it passes through a keyhole on 2029 April 13; this keyhole is a region in space approximately 4.6 km wide lying within $5.7736–5.7744\,R_\oplus$ of the Earth's geocentre. Another dangerous possibility is that Apophis will pass through a second 6.4-km-wide keyhole lying within $6.3395–6.3405\,R_\oplus$ of the Earth's geocentre. This last one would lead to a collision in 2037 April. We also determined a few other extremely small keyholes leading to impacts after 2037. These keyhole ranges were obtained using extensive Monte Carlo simulations. A large samples of virtual asteroids (hereafter VAs) in a full six-dimensional uncertainty region of orbital elements (or position–velocity region) have been generated. Thus, the analysis has been constrained to a pure ballistic problem. A similar approach was applied by Giorgini et al. (2008), who used the Monte Carlo method in six-dimensional position–velocity space. They examined the Apophis positional uncertainty after 2029, but did not investigate the Apophis impact orbits.

The equations of the asteroid's motion have been integrated numerically using the recurrent power series method (Sitarski 1989, 2002), taking the perturbations by all the planets and by the Moon into account and also including relativistic effects and second-order terms (Sitarski 1979) when searching for impact orbits. The perturbations from the four largest asteroids (Ceres, Pallas, Vesta, Hygiea)

[2] The term keyhole is used here according to its classical meaning introduced by Chodas (1999). This term may also be used to indicate a region on the target plane of the first encounter leading (at a subsequent return) not necessarily to a collision but to a deep encounter (for more details see Valsecchi et al. 2003).

Table 2. Orbital models for Apophis. Models A, B, C, D and E/E′ differ in the assumed criterion of selection. The data for the first three models were processed without weighting, whereas the latter two included weighting. In column 5, threshold values of rms for the confidence level $\alpha = 0.99$ are given (see Section 3 for details).

Model	Observational interval	Number of residuals	rms (arcsec)	rms_{99} (arcsec)	K	γ_1	Minimal distance on 2029 April 13 [$R_\oplus$]	Impact probability in 2036	Impact probability in 2037
Solar system dynamical model without four most massive asteroids									
A	2004 03 15 – 2006 08 16	1964	0.416	0.418	1.3	−0.12	6.151 ± 0.155	1.4×10^{-5}	9.6×10^{-5}
B	2004 03 15 – 2006 08 16	1950	0.399	0.400	0.9	−0.13	6.066 ± 0.149	6×10^{-6}	4×10^{-6}
C	2004 03 15 – 2006 08 16	1424	0.262	0.263	−0.1	−0.10	5.956 ± 0.106	1.3×10^{-5}	$\sim 10^{-7}$
D	2004 03 15 – 2006 08 16	1980	0.316	0.317	0.2	−0.12	6.074 ± 0.083	5×10^{-7}	1.9×10^{-6}
E	2004 03 15 – 2006 08 16	1971	0.308	0.309	−0.1	−0.10	6.065 ± 0.081	6×10^{-7}	2.0×10^{-6}
Including four most massive asteroids									
E′	2004 03 15 – 2006 08 16	1971	0.308	0.309	−0.1	−0.10	6.064 ± 0.095	7×10^{-7}	1.8×10^{-6}

are included only for model E′. This allows us to estimate the influence of these objects on the impact risk probability. All numerical calculations presented here are based on the Warsaw numerical ephemeris DE405/WAW of the Solar system, consistent with a high accuracy with the JPL ephemeris DE405 (Sitarski 2002). The positional observations of Apophis are taken from the NEODyS pages publicly available at http://newton.dm.unipi.it/neodys/.

2 SELECTION AND WEIGHTING OF ASTROMETRIC OBSERVATIONS

The selection and weighting of astrometric observations constitute a crucial procedure in the determination of the asteroid orbit. Different groups use different methods of data preparation. For example, in the case of Apophis, researchers from the Jet Propulsion Laboratory rejected about 26 per cent of the optical measurements. The resulting rms from 738 optical measurements and 7 radar observations is reduced to 0.352 arcsec. Similarly, Giorgini et al. (2008), who rejected about 21 per cent of the optical data and kept 7 radar measurements, determined the nominal orbit with an rms of 0.407 arcsec. One widely used method of data selection and weighting – 'global residual statistics' – is described by Carpino, Milani & Chesley (2003). It is based on the global O−C statistics of the optical astrometric observations collected for about 17 000 numbered asteroids. The 'global weights' are used for an automatic orbital analysis of asteroids by many authors. This method was applied for Apophis by researchers at the Near Earth Objects – Dynamic Site. Five out of 1000 astrometric observations were rejected and 264 measurements were 'downweighted' by a factor of 100 (meaning that in effect only 731 observations were used), resulting in an rms of 0.302 arcsec (the radar data were also included). However, an inspection of the details of the data processing shows that for 68 per cent of optical observations the weights have the attribute 'forced', which implies that 'manual' intervention has been applied to the majority of observations.[3]

Similarly to Carpino et al. (2003), we use the objective statistical method; however, we treated the existing set of observations of each individual asteroid as the unique one. In fact, we have used our method (the details of which are still being improved) for more than 20 years, and hence we give here only a brief description of the criteria used for the statistical analysis of data. According to our method, we subdivide each data set of a given asteroid into oppositions, and within each opposition, into observatories. Thus, according to the relative differences in O−C we construct the relative and normalized weights for each observatory and each opposition for a given asteroid. To avoid problems with the oppositions being overpopulated with many series of data taken close together in time in comparison to the older oppositions, we can construct so-called 'normal places' by replacing several observations on the same day (that is, taken by a single observatory) by one average asteroid position. In the case of Apophis, however, this was not necessary.

To investigate the influence of the data selection and weighting on the existence of impact orbits, especially on the probability of impact with the Earth, we prepared the first two sets of observations applying Bielicki's and Chauvenet's criteria for selection, and treating all the data points as equivalent observations (models A and B, respectively; see Table 2). The criteria differ in the upper limit of the accepted residuals, ξ, that is, observed minus computed values of right ascension, $\Delta\alpha \cos\delta$, and declination, $\Delta\delta$. According to Chauvenet's criterion (Chauvenet 1908), from the set of N residuals, ξ, we should discard all values of ξ for which

$$| \xi | > \sigma \, K_{1/2}(N),$$

where σ is the dispersion of ξ,

$$\sigma = \sqrt{\left(\sum_k \xi_k^2 \right) / N},$$

and $K_{1/2}(N)$ is the unknown upper limit of the integral of the probability distribution, $\phi(\xi)$:

$$\int_0^{K_{1/2}} \phi(x) \mathrm{d}x = 1 - \frac{1}{2N},$$

where $x = \xi/\sigma$.

According to this criterion, a data point is rejected if the probability of obtaining the particular deviation of residuals from the mean value is less than $1/(2N)$. To determine this probability a normal distribution of ξ is assumed.

In the less restrictive Bielicki criterion (Bielicki 1972), data points are rejected if

$$| \xi | > \xi_{K_B} = \sigma \, K_{1/2}(N)/(1 - 0.4769363\sqrt{N}).$$

It is taken into account here that the dispersion σ itself is a random variable.

[3] This is in contrast to the information on the web page stating that such data handling is rarely applied.

We also used the Bessel criterion, which is more restrictive than Chauvenet's criterion. The Bessel criterion rejects from the set of N residuals all the values of ξ for which

$$|\ \xi\ | > \sigma\ K_1(N)\,,$$

where $K_1(N)$ is defined by

$$\int_0^{K_1} \phi(\xi)\mathrm{d}\xi = 1 - \frac{1}{N}.$$

To reduce systematic errors in the observational material, such as the bias associated with a site as a function of time, one should consider specific procedures. In the present investigation we divided the whole observational material into several time subintervals according to the inertial structure of the material (i.e. according to existing gaps in the observations).

The application of Chauvenet's criterion to the Apophis data resulted in the rejection of 14 more residuals than the use of Bielicki's criterion (models A and B in Table 2, column 3). Our selection method allows us to discard any 'bad' residual in right ascension, keeping the 'good' residual in declination, and vice versa. In the set of the Apophis observations, the Bessel criterion resulted in the rejection of only a few residuals more than did Chauvenet's criterion. To visualize the importance of the data selection we constructed model C, in which we arbitrarily removed all the residuals with O−C greater than 0.6 arcsec. It is important to stress that ignoring some statistically acceptable data points (in this case about 29 per cent of all the observations) can affect the data in statistically unacceptable way. The fact that, owing to the smallest rms value, model C looks more attractive than model A and model B cannot be used as an argument favouring this model.

Next, two sets of data (models D and E) were handled by the iterative procedure of selection and weighting of the observations. At the end of the iteration the computed weights were normalized to unity for all the observers. This procedure has been described in detail by Bielicki & Sitarski (1991). Model D is based on Bielicki's criterion of selection, and model E, on Chauvenet's criterion. It can be seen from Table 2 that the weighting and selection procedure leads to significantly smaller mean residuals and restores more data than the selection procedure alone.

After fitting the Gaussian model to the O−C distributions for all five nominal orbits we concluded that the distributions of residuals for the two non-weighted models A and B show some deviations from the Gaussian model. These deviations can be described by the kurtosis, K (related to the fourth moment of the distribution), and skewness, γ_1 (related to the third moment). We use standard definitions of both quantities: $K = (\mu_4/\sigma^4) - 3$, where μ_4 is the fourth central moment and σ is the standard deviation, and $\gamma_1 = (\mu_3/\sigma^3)$, where μ_3 is the third central moment.

The values of kurtosis and skewness are given in Table 2. The amplitudes of skewness at about −0.1 for the O−C distributions in the case of the non-weighted data (models A and B) indicate that these distributions are satisfactorily symmetric. However, the kurtosis for these samples is equal to 1.3 and 0.9, respectively. Thus, these distributions are leptokurtic – with a distinct peak at the mean as compared with the Gaussian distribution (Fig. 1). This means that the classical assumption that the observation errors are distributed according to the Gaussian probability density function is not true in the case of Apophis.

According to the assumption incorporated in the weighting procedure, the weighted O−C distributions are normal; that is, values of kurtosis are close to zero (see models D and E in Table 2 and Fig. 1). When all the residuals greater than the arbitrarily assumed limit of 0.6 arcsec were rejected, a Gaussian O−C distribution was obtained (model C).

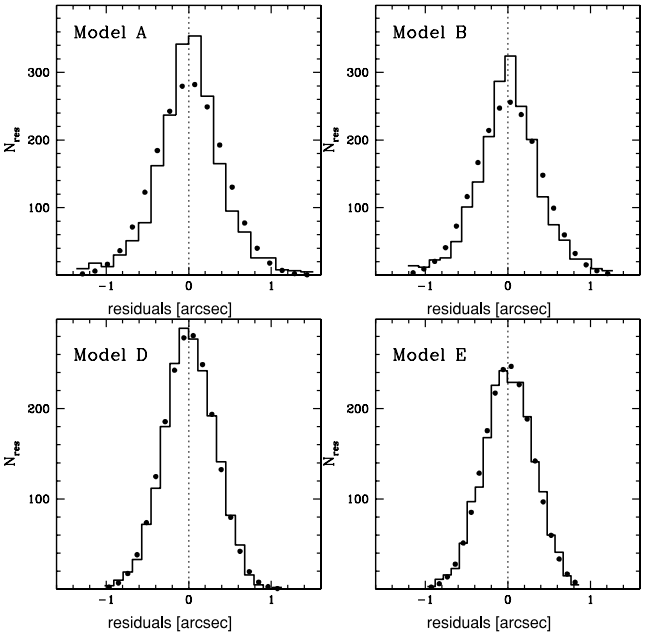

Figure 1. The O−C distributions for the non-weighted data (upper panel, models A, B) and the weighted data (lower panel, models D, E). The best-fitting Gaussian distributions are shown by black dots.

Using two types of procedure, selection without weighting (models A–C) and with weighting (models D and E), we have determined by means of the least-squares method the best-fitting osculating orbits (hereafter nominal orbits), which are now used as a basis for our impact investigation.

2.1 Comparison of the nominal orbit with other orbital solutions

To compare our solutions with the analogous results in the literature, we also determined the nominal orbital elements of model E for the epochs given by Giorgini et al. (2008), Vinogradova et al. (2008) and two well-known Web sources: the JPL Small-Body Data base and Near Earth Objects – Dynamic Site (NEODyS) (see Table 3). In all these four sources the 7 radar measurements have been incorporated into the orbital determinations. We concluded that our values of uncertainties are in excellent agreement with those results, except for the uncertainty in the anomaly given by Giorgini et al. (2008), which is an order of magnitude smaller than the uncertainties determined by all the remaining groups, including ours. Our values of the nominal orbital elements are consistent within 3 sigma with the results obtained by the other groups (see also the Appendix).

3 CLONING OF THE NOMINAL ORBIT

To analyse the impact possibilities in the consecutive encounters of Apophis with the Earth, it is necessary to examine the evolution of any possible orbit of Apophis from the confidence region; that is, from the six-dimensional region of orbital elements where each set of orbital elements is compatible with the observations. We construct the confidence region using the Sitarski method of random orbit selection (Sitarski 1998).

Table 3. Comparison of selection and weighting methods implemented by various groups for 1000 optical observations of Apophis in the time interval 2004 03 15–2006 08 16. Columns 2 and 3 give in parentheses the number and percentage of measurements downweighted by a factor of 100; in column 5, 'no?' denotes our assessment based on the large number of discarded observations and the value of rms.

Source	Number of used optical obs.	Percentage of of discarded optical obs.	Number of used radar obs.	weighting of obs.	rms (arcsec)
Giorgini et al. (2008)	792	21	7	no?	0.407
Vinogradova et al. (2008)	956	4.5	7	no	0.370
JPL SBD	738	26	7	no?	0.352
NEODyS	995 (264)	0.5 (26)	7	yes	0.302

The Sitarski method allows us to generate any number of randomly selected orbits of VAs, which in the Apophis case represents the observations with almost the same value of rms as the nominal orbit (to within 0.002 arcsec for 99 per cent of VAs). It should be noted that, according to our random selection method, the derived sample of VAs follows the normal distribution in the orbital elements space. Furthermore, the rmss fulfil the six-dimensional normal statistics. According to the chi-square test of significance we have:

$$(\mathrm{rms}_i)^2 = (\mathrm{rms}_{\mathrm{nom}})^2 \left[1 + \Delta_\alpha \chi^2 / \chi^2_{\mathrm{min}}\right] i = 1, ...N\,,$$

where the increment $\Delta_\alpha \chi^2$ is defined by standard χ^2-statistics for the selected confidence level, α, and the relevant number of 'interesting' parameters, N_p, that is, the number of parameters estimated simultaneously (Avni 1976). Because the χ^2-values are calculated using the sample dispersions, σ, the minimum $\chi^2_{\mathrm{min}} = N - N_\mathrm{p}$, and in our case $N_\mathrm{p} = 6$, because six orbital elements have been simultaneously drawn in the selection of the cloned orbits.

Critical values of $\Delta_\alpha \chi^2$ can be found in statistical tables. For example, for a chi-square distribution with six interesting parameters we obtain 90 per cent of clones with $\Delta_\alpha \chi^2 < 10.645$ and 99 per cent of clones with $\Delta_\alpha \chi^2 < 16.812$. This means that the rms of a true (unknown) orbit of Apophis should satisfy the inequality

$$\mathrm{rms}_{\mathrm{true}} \leq \mathrm{rms}_{99} = \mathrm{rms}_{\mathrm{nom}} \sqrt{1 + 16.812/(N-6)}$$

for a confidence level of 99 per cent. The rms_{99} values are listed in column 5 of Table 2.

It can be seen from Fig. 2 that the orbital cloning procedure at the epoch relatively close to the observational arc provides an excellent agreement between the derived rms distribution (solid curve) and the theoretical six-dimensional normal distribution (crosses). The same procedure applied for the epoch of 2029 01 29 gives a more dispersed sample of cloned orbits (the dashed curve), mostly as a result of tiny differences in the planetary perturbations for the individual orbital clones. When the sample of clones selected in 2006 was integrated to the epoch in 2029 a similar dispersion was observed.

The randomly selected orbits form the confidence region in the six-dimensional space of possible osculating elements, and the dispersion of each orbital element is given by its uncertainty estimated from the least-squares method of the orbit determination.

Fig. 3 shows the orbital element distributions of a sample of 15 000 VAs for the orbital solution represented by the nominal orbit of model A, and Fig. 4 presents projections of the six-dimensional parameter space of 15 000 virtual orbits of Apophis on to the plane of two chosen orbital elements. The orbital cloning procedure was applied at the epoch of 2006 09 22, close to the observational arc. The derived swarm of VAs follows the normal distribution in the six-dimensional space of orbital elements. This is visualized by four grey tints of points in Fig. 4. Each point represents a single virtual orbit, and its grey tint indicates the deviation magnitude from the nominal orbit with confidence levels of: <50 per cent, 50–90 per cent, 90–99 per cent and >99 per cent (from the biggest and darkest grey points to the smallest and lightest grey points, respectively). The symbols in the crowded areas overlap heavily, and the darkest points are often covered by lighter points.

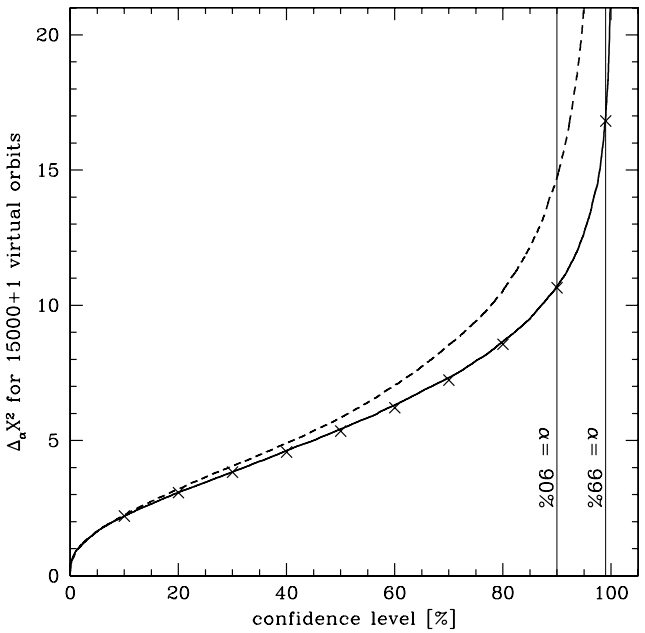

Figure 2. $\Delta_\alpha \chi^2$ for the sample of 15 000 clones derived in model A. Statistics of the sample of cloned orbits generated at the epoch of 2006 09 22 are shown with a solid curve, and the $\Delta_\alpha \chi^2$ distribution of the sample of clones generated at the epoch of 2029 01 24 (three months before 'keyhole' passage) is dashed. Grey vertical lines represent the confidence levels of 90 and 99 per cent, respectively.

A comparison between the orbital element distributions in all five models is given in Fig. 5 for the semimajor axis (upper panel) and the mean anomaly (bottom panel).

4 IMPACT ANALYSIS OF APOPHIS: METHOD AND RESULTS

We are able to determine directly the sample of impact orbits for each close encounter with the Earth whenever such risk orbits exist (Sitarski 2002). However, we have developed a new method to analyse the impact probability.

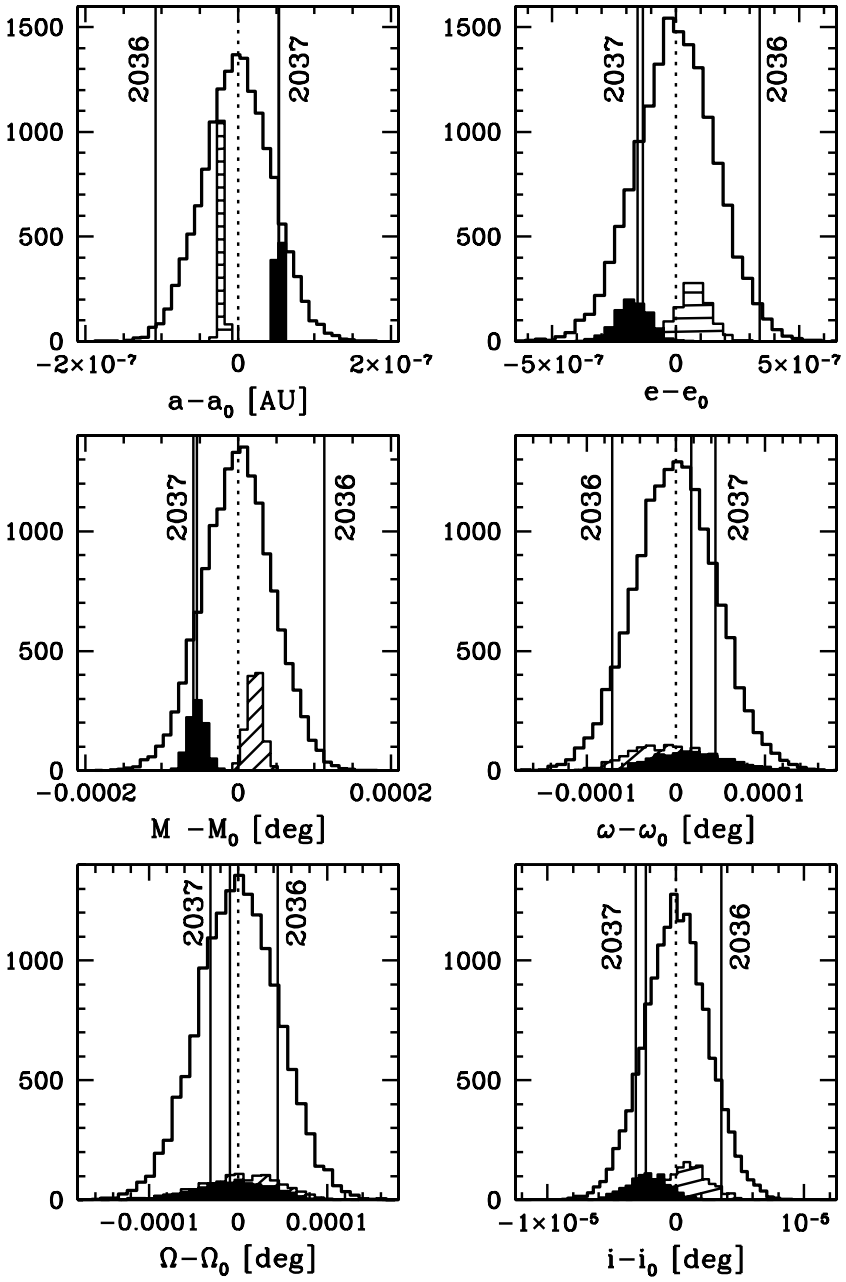

Figure 3. The distribution of possible osculating orbits of Apophis obtained for model A. The sample of 15 000 virtual orbits was generated for the epoch of 2006 09 22. The plot is centred on the values of orbital elements of the nominal osculating orbit (epoch: 2006 09 22), represented by dotted vertical lines. Distributions of VAs that pass closer than 0.04 au in 2037 April (ascending node) and 2037 September (descending node) are given by filled and dashed-filled histograms, respectively. The three impact orbits derived from this sample are shown by the solid vertical lines (one impact orbit in 2036, and two in 2037).

To examine the close encounter of Apophis with the Earth in 2029 and the risk of impact in the following years, a non-linear two-stage analysis was performed numerically.

In the first step, we constructed a sample of 15 000 clones (15 000 VAs) (see Section 3) for each of the orbital solutions described in Table 2. Each of these orbital clones was then integrated forwards in time to the year 2100. Thus, we integrate the swarm of VAs from the whole uncertainty region, not only the VAs lying on the line of variations (LOV). Furthermore, our swarm of VAs follows a normal distribution in orbital elements space.

From these 90 000 VAs we obtained three impact orbits for model A (one in 2036 and two in 2037) and one impact orbit for model B (in 2036). We also note that about 6–7 per cent of VAs (depending on the model) passed Earth in 2051 April within a distance of ∼0.000069–0.04 au. The vertical lines in Fig. 3 represent the positions of impact orbits in the sample of 15 000 clones in model A, and the positions of impact orbits in the semimajor distributions and mean anomaly distributions for all five models are shown in Fig. 5. It can be seen from Fig. 3 that the range of semimajor axes including all the clones passing closer than 0.04 au from the geocentre (filled histogram) in 2037 is relatively narrow in comparison with the full a-distribution. Analogous ranges for the remaining orbital elements are more dispersed.

In the second step, on the basis of the obtained impact orbits (four orbits in this example), we construct the potentially 'dangerous' intervals of semimajor axes at our epoch of orbital cloning

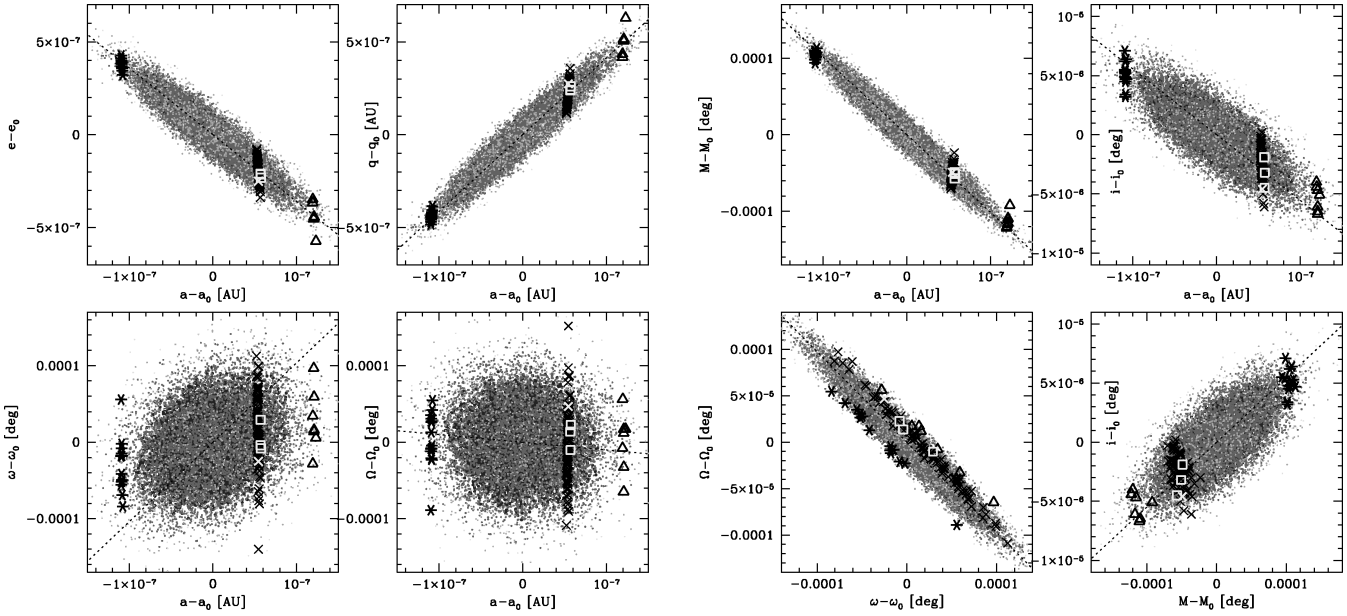

Figure 4. Projection of the six-dimensional space of 15 000 possible osculating orbits of Apophis on to the plane of two chosen orbital elements (model A). Each point represents a single virtual orbit, and the grey tints indicate the deviation magnitude from the nominal orbit with confidence levels of: <50, 50–90, 90–99 and >99 per cent (from the darkest grey to the lightest grey, respectively). Lines of variations are given by black dotted lines. The impact orbits are shown by black crosses (impact in 2037), black asterisks (impact in 2036) and triangles (2046). The derived impact orbits for the year 2054 (light grey squares) and 2059 (light grey crosses) are superimposed on the background of black crosses. Each individual plot is centred on the nominal values of the respective pair of orbital elements denoted by the subscript '0' (epoch: 2006 09 22).

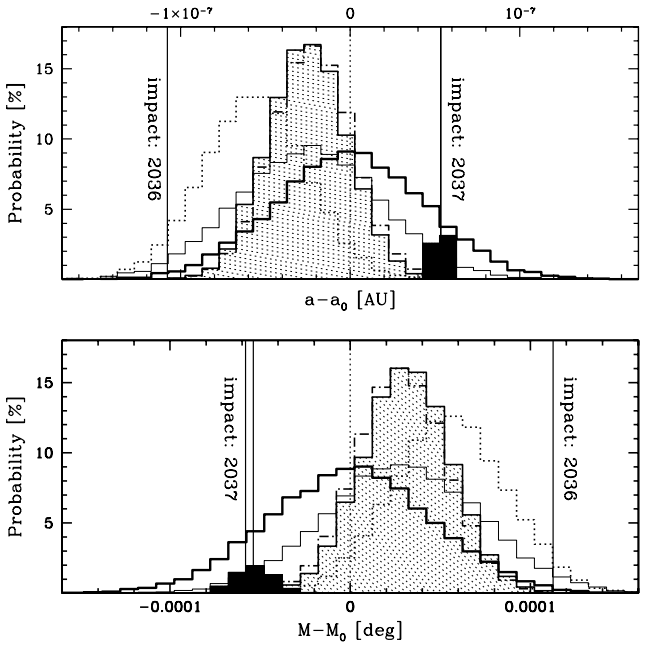

Figure 5. Distributions of the semimajor axes (top panel) and mean anomalies (bottom panel) derived in models: A, thick solid-line histogram; B, thin solid-line histogram; C, dotted-line histogram; D, dash–dotted line; E, filled histogram. Each distribution was constructed on the basis of the samples of 15 000 virtual orbits (epoch 2006 09 22) and is centred on the nominal value of the semimajor axis (top panel) and mean anomaly (bottom panel) derived in model A. The three impact orbits derived in model A from the sample of 15 000 clones are given as vertical lines (one impact orbit on 2036 April 13 and two impact orbits on 2037 April 13). Distributions of clones that pass closer than 0.04 au in 2037 April are denoted by filled black histograms.

(2006 09 22). The 'dangerous' ranges of semimajor axes were also independently derived for all dates of potential impacts or close encounters using the Sitarski method (Sitarski 2006). In this way we are able to randomly select large numbers of VAs (for each model of data selection and weighting) and then for the numerical integration take only VAs within a 'dangerous' interval for the given moment of impact. After many tests it turned out that these 'dangerous' intervals are very narrow in the a-distribution. Thus, to evaluate the true probability of the impact, it was possible to randomly select millions of clones and then effectively integrate only a thousand or dozens of thousands of clones. It is important to stress here that the impact probabilities given in Table 2 were always estimated from samples of at least one million randomly selected VAs. Finally, we detected 96 impact orbits in 2037 April and 14 impact orbits in 2036 April in model A (non-weighted observations, sample of one million VAs). We also detected impact orbits in 2036 in model B (6 events) and in model C (13 events), whereas in models D and E we have no impact orbit in 2036 from the sample of one million randomly selected orbits. However, in the sample of 10 million VAs, five and six impact VAs in 2036 were detected (in models D and E, respectively), and 19 and 20 impact VAs in 2037.

These results can be qualitatively explained by the positions of impact orbits relative to the a-distribution in the top panel of Fig. 5. The semimajor axis a_0 of the nominal orbit of model A has been selected as a reference value on the abscissa for all five models. For this reason, the histograms for models B to E are displaced from the central position. Solid vertical lines indicate the semimajor axes of the impact orbits, and one can see why for the weighted observations (models D and E) the impacts in 2036 and 2037 have a significantly lower probability than those for models A and B (obviously, the histograms for 15 000 VAs are not representative for the wings of the distributions of 1–10 million VAs).

Table 4. Keyholes for the potential impacts in 2036, 2037, 2046 and impacts in 2044, 2054, 2055, 2056, 2059, 2076 that are preceded by a close encounter with Earth in 2036, 2037, 2046 or 2051

Potential impact in April:	Keyhole at the epoch of 2029 04 13 [$R_\odot$]	Impact probability Model A	Model B	Model C	Model D	Model E
2036	5.7736–5.7744	1.4×10^{-5}	0.6×10^{-5}	1.3×10^{-5}	5×10^{-7}	6×10^{-7}
2053	5.7763	$< 10^{-6}$	$< 10^{-6}$	$< 10^{-6}$	$\sim 10^{-7}$	$< 10^{-7}$
2076	5.97347	$\sim 10^{-6}$	$<10^{-6}$	$<10^{-6}$	$< 10^{-7}$	$\sim 10^{-7}$
2059	∼6.3359	$\sim 10^{-6}$	$<10^{-6}$	$<10^{-6}$	$<10^{-7}$	$<10^{-7}$
2044	∼6.3370	$< 10^{-6}$	$<10^{-6}$	$<10^{-6}$	$\sim 10^{-7}$	$\sim 10^{-7}$
2037	6.3395–6.3405	9.6×10^{-5}	4×10^{-6}	$\sim 10^{-7}$	1.9×10^{-6}	2.0×10^{-6}
2056	6.3426	$< 10^{-6}$	$<10^{-6}$	$<10^{-6}$	$<10^{-7}$	$<10^{-7}$
2054	6.3486–6.3488	3×10^{-6}	$<10^{-6}$	$<10^{-6}$	3×10^{-7}	$\sim 10^{-7}$
2046	6.5702–6.5706	8×10^{-6}	$<10^{-6}$	$\ll 10^{-6}$	$\ll 10^{-7}$	$\ll 10^{-7}$
2055	∼6.5739	2×10^{-6}	$<10^{-6}$	$\ll 10^{-6}$	$\ll 10^{-7}$	$\ll 10^{-7}$

In addition, the probability of about 8×10^{-6} for an impact in 2046 was estimated in model A (8 impact orbits from one million clones). On the basis of these 8 impact orbits we calculated a keyhole of width 2.9 km at a distance of 6.5702– 6.5706 $R_\oplus$ from the Earth's centre on 2029 April 13 (Table 4).

A careful analysis of the VA orbits has revealed several interesting new results. When we examined the 'dangerous' interval for the impact risk in 2037, we detected a series of impacts in the years following 2037. First, we found two new keyholes on 2029 April 13 – closely related to the 2037 keyhole: a keyhole of width ∼1.3 km lying at a distance of 6.3486–6.3488 $R_\oplus$ from the Earth's centre (calculated from three impact orbits in 2054), and a keyhole at a geocentre distance of ∼6.3359 $R_\oplus$ (estimated from one impact orbit in 2059). Second, we derived a particular impact orbit in 2076 connected with a very close encounter with Earth in 2051. In our basic samples, as mentioned above, about 6–7 per cent of VAs (depending on the model) passed Earth at a distance of ∼0.000069–0.04 au. However, only those VAs that pass near the Earth at a distance of almost exactly ∼0.00819 au in 2051 have a chance of hitting the Earth in 2076. Because the keyhole in 2029 is extremely narrow for impact in 2076, the probability of this impact is lower than the probability of impact in 2036, although the VAs hitting the Earth in 2076 are much closer to the nominal orbit than the VAs hitting the Earth in 2036.

Detected impact orbits from the swarm of one million VAs are shown in Fig. 4 superimposed on the sample of 15 000 VAs constructed for model A in the first step of our analysis. It can be seen that each projection of the impact VAs on to a plane of a pair of orbital elements forms an elongated structure for a given impact date. It should be noted that these structures generally (although not always) intersect the LOV projection (Fig. 4). Thus, if the search is limited to this line, some impact orbits would be found. Nevertheless, most of the impact orbits are situated far from the LOV, and to find all the possibilities of impact orbits one should examine the entire six-dimensional volume of the orbital element space.

A comparison between the swarms of 15 000 VAs derived in models A, B and E′ and the impact VAs in these three models detected in 1–10 million VAs is shown in Fig. 6.

4.1 Trajectory prediction uncertainty at the moment of close encounter in 2029

The probability distributions of the encounter distance with the Earth on 2029 April 13 are shown in Fig. 7 for all five models of data processing. Each histogram was constructed for 15 000 VAs. The expected values of the Apophis encounter distance with the Earth are calculated by fitting the normal distribution to each of these histograms. The results are given in column 8 of Table 2. The weighted mean value of the geocentric encounter distance calculated from all five minimal distance estimations is equal to $6.055 \pm 0.099\ R_\oplus$.

It can be seen that the inclusion of the four most massive asteroids in the Solar system dynamical model makes the distribution of the minimal distance during the close-encounter event in 2029 wider by about 17 per cent (compare model E and model E′; the selection and weighting of data are the same in both models). According to Giorgini et al. (2008) these four asteroids constitute about 68 per cent of all the asteroid perturbers during 2004–2036. Thus, to account for all asteroid perburbers we expect that this minimal distance distribution in 2029 becomes wider by an additional ∼8 per cent, giving $\sigma \simeq 0.101\ R_\oplus$ in the case of model E. However, we obtained quite similar probabilities for the impacts in 2036 (6×10^{-7} and 7×10^{-7}) and 2037 (2.0×10^{-6} and 1.8×10^{-6}) in both models (E and E′). Once again, specific features of the investigated events indicate the significance of non-linear effects in the impact analysis of Apophis. For example, in model E we derive one impact VA in 2044 (from the sample of 10 millions VAs; not shown in Fig. 7) that previously passed close to the Earth in 2037, whereas in model E′ we also derive one impact VA in 2044; however, this VA passed near the Earth in 2036. It was found that the first impact clone was placed in the right wing of the 2029 keyhole distribution in model E (Fig. 7), whereas the second was placed in the left wing of the keyhole distribution in model E′ (notice that both minimal distance distributions are centred on the same value of 6.06 $R_\oplus$).

Table 2 and Fig. 7 show that models based on the weighted observations are the most accurate and very similar. The best (from a statistical point of view) solutions give a geocentric encounter distance of $6.065 \pm 0.081\ R_\oplus$ (model E) or $6.064 \pm 0.095\ R_\oplus$ (model

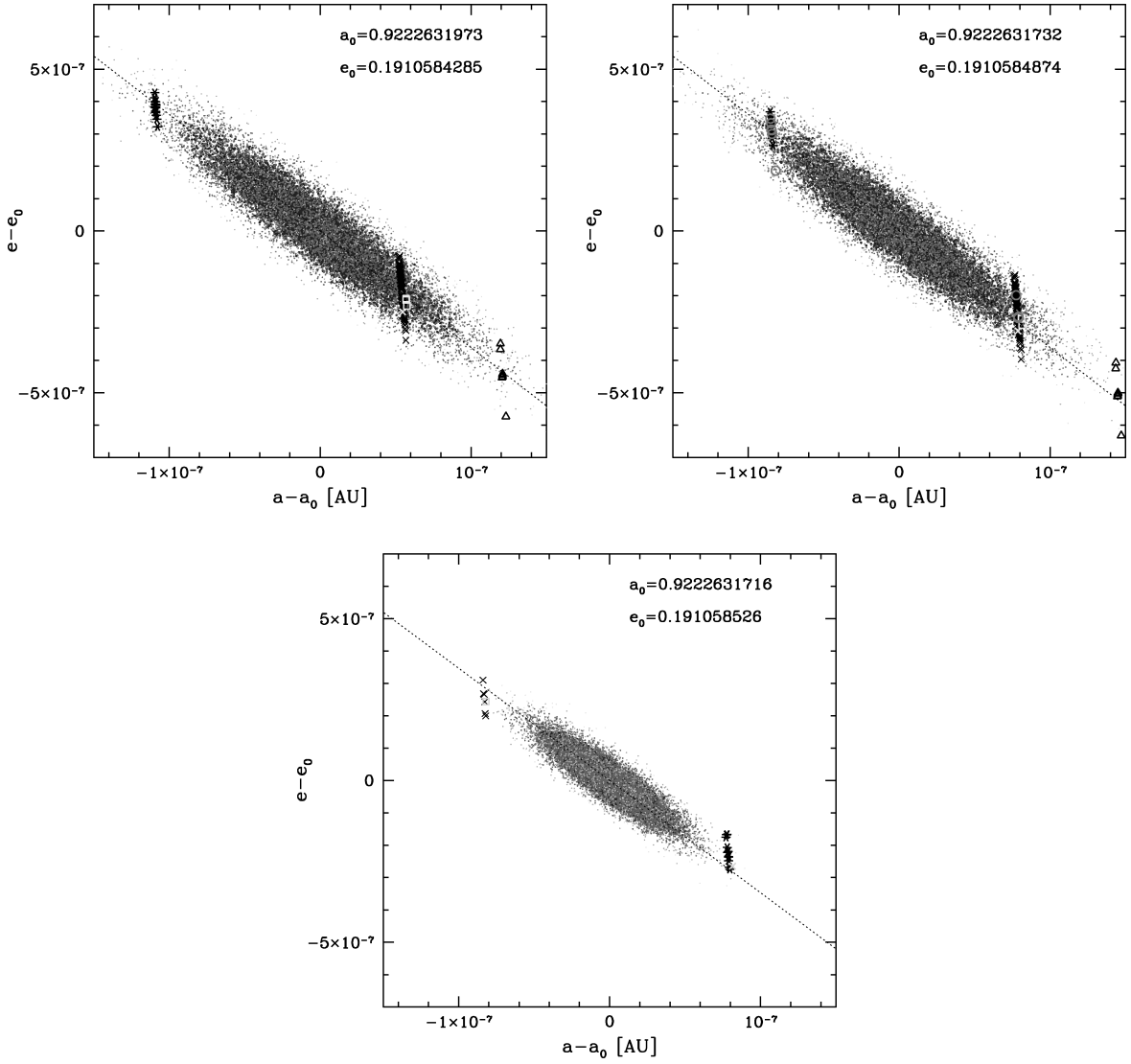

Figure 6. Projection on to the *a–e* plane in the six-dimensional space of possible osculating orbits of Apophis obtained for model A (upper left panel), B (upper right panel) and E′ (lower panel). Samples of 15 000 VAs are given by points coded as in Fig. 4. All derived impact orbits in model A (from one million VAs) are shown in both upper panels with the same symbols as in Fig. 4. The impact VAs derived in model B (impacts in 2036 and 2037 detected from one million VAs) are shown with grey open circles in the right upper panel (on the background of impact VAs from model A), and the impact orbits derived in model E′ (impacts from 10 million VAs) are shown in the bottom panel (light cross, one impact VA in 2054 on the background of 18 impact VAs in 2036; light square, one impact VA in 2044 on the background of seven impact VAs in 2036). Each plot is centred on the values of the semimajor axis, a_0, and eccentricity, e_0, of the nominal orbit given in the right corners of each plot (epoch: 2006 09 22).

E′) on 2029 April 13. Both values are in excellent agreement with the $5.96 \pm 0.09\,R_\oplus$ given by Giorgini et al. (2008) as the best estimate of the geocentric encounter predicted from the optical observations *and* the radar measurements.

Table 4 presents the range of distances from the Earth of all the numerically detected impact keyholes at the moment of the close encounter with the Earth on 2029 April 13. The keyholes that were detected in model A from one million VAs are shown by vertical lines in Fig. 7. It is important to stress that the symbols $<10^{-6}$ (or $<10^{-7}$) given in Table 4 denote only that we did not find any impacts in one million (10 million) VAs. It should be noted that in the case of the non-weighted data (models A–C) we performed analysis based on one million VAs, whereas for the weighted models (models D, E and E′) the analysis was based on 10 million VAs.

Inclusion of the four most massive asteroids in the Solar system dynamical model does not affect significantly the position of the 2029 April 13 keyholes for the impacts in 2036, 2037 and 2046. However, the impacts in all the remaining years listed in Table 4 followed after the close encounter of the VA with the Earth. Therefore, the evolution of such VAs is very sensitive even to the very small additional perturbations, including the perturbations from the massive asteroids. An example of such a perturbation was discussed in this section in the context of the impact orbit in 2044.

4.2 Impact orbits far from the nominal orbit of Apophis

By analysing the impact possibilities based on the shorter arcs of observations (see arc3 and arc5 in Table 1) we derived many impact orbits in 2048 and many other impact possibilities for the following

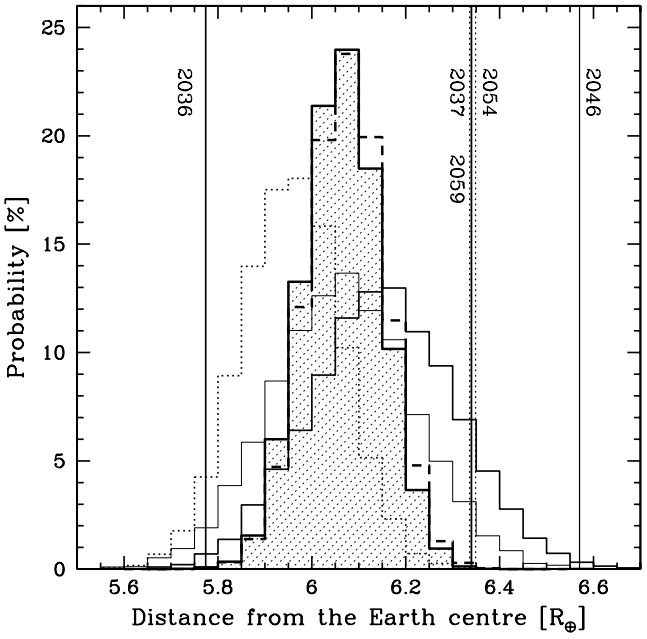

Figure 7. Distributions of the minimum distance of the asteroid Apophis from the centre of the Earth on 2029 April 13 derived for the samples of 15 000 virtual orbits. The minimum-distance histogram for model A is shown with a thick solid line, for model B with a thin solid line, for model C with a thin dotted line, and for model D with a thick dashed histogram. For the most accurate model E, the distribution is shown with a thick solid line and filled histogram. Distances for selected impacts at dates indicated by labels are shown.

years (2049, 2062, 2063, 2065) that are connected with the close encounter in 2048. According to the present interval of observations, all these impact events are practically excluded because they would take place if Apophis passed near the Earth in 2029 at a distance of 7.060–7.063 $R_\oplus$. It can be seen from Fig. 7 that this keyhole for impact in 2048 is on the far left wing of the displayed distributions for the current orbital models of Apophis. Still further out on the left wing in Fig. 7 are the keyholes for impacts in 2053 and 2067 discussed by Sitarski (2006) on the basis of the non-weighted data.

4.3 Orbital evolution of Apophis after 2029

During the incoming first close encounter with the Earth on 2029 April 13, the orbit of Apophis will change. The most significant change from 0.92 to 1.10 au will affect the semimajor axis.

In the top rows in Figs 8 and 9 the distributions of six orbital elements at the epoch of 2029 05 08 are shown for model A. Apparently, after the close encounter on 2029 April 13, the distributions of parameters of the clone swarms are still close to the normal distributions, although with dispersions several orders of magnitude greater than those for the swarm drawn for the epoch 2006 09 22 (Figs 3 and 5), or any epoch before the close encounter in 2029 April. By comparing the dispersions of semimajor axes (perihelion distance) we have found that the dispersion increases by five orders of magnitude from $\sim 4.5 \times 10^{-8}$ au $\simeq 6.7$ km ($\sim 2 \times 10^{-8}$ au $\simeq 3$ km) at the epoch of 2029 01 24 to $\sim 5 \times 10^{-3}$ au ($\sim 2.5 \times 10^{-3}$ au) at the epoch of 2029 05 08. Generally, an ellipsoid of the orbit uncertainty grows in each orbital element by at least four orders of magnitude as a result of the close encounter with the Earth on 2029 April 13. It should be noted that the range of semimajor axes for impact VAs in 2036 (in 2037) also changes dramatically during the close encounter in 2029, from 0.68 km (1.2 km) on April 10 to 2070 km (2190 km) on April 14.

It is interesting that our model C, with the smallest rms (Table 2), gives exactly the same minimal distance of the nominal orbit on 2029 April 13 as Giorgini et al. (2008), who give a minimal distance of $5.96 \pm 0.09\,R_\oplus$. However, in model C no weighting was applied, and almost 29 per cent of the optical data were discarded. Because we believe that such extensive rejections of the modern data are groundless, we consider our model E better than model C in the statistical sense. We found that in model E the uncertainty along the orbit path on 2036 April 13 is analogous to those presented in fig. 4 of Giorgini et al. (2008) (10 000 VAs).

After the close encounter in 2029, the distributions of orbital elements are not adequately described by the normal distributions. Consecutive returns to the Earth significantly change the orbital elements of those clones that pass through the small keyholes in 2036 and 2037. This is demonstrated by the distribution of the semimajor axes and the eccentricities for model A (the first and second columns in Fig. 8, respectively). In the first row the positions of the impact clones in 2036 April and in 2037 April (solid vertical lines) are shown. The subsample of clones that pass closer than 0.04 au in 2037 April are represented by filled histograms. In 2036 May (second row in Fig. 8) there is a deficit in the Gaussian shape around the position of the impact orbit in 2036. This results from the Earth's perturbations, which have changed the orbits of these clones significantly. A second and very prominent dip appears in 2037 May at the position of the subsample of clones that in 2037 April passed closest to the Earth. It can be seen that these clones were almost completely removed from the narrow interval of semimajor axis and eccentricity and were dispersed over the rest of the histogram (filled distributions in the third row in Fig. 8). Distributions derived in 2052 May display many similar dips that were created by the periodic relatively strong perturbations of the Earth (between 2037 and 2052) that affect different parts of distributions.

5 SUMMARY AND CONCLUSIONS

Although the motion of Apophis can be well predicted before its deep close encounter with the Earth on 2029 April 13, the present observations are not adequate to eliminate definitely the possibility of impact with the Earth in 2036 and in many years following this, even in a fully ballistic model. It seems that the seven available radar measurements are not crucial at present for the nominal orbit determination, although historically they were important for indicating that the pre-discovery observations of 2004 March were biased by some systematic errors. It is important to stress that future radar observations will be important to draw conclusions concerning impacts in 2036 and impacts following 2036. In the present paper we inspected the optical astrometric observational material carefully. Our best solution for the passage on 2029 April 13 gives a geocentric encounter distance of $6.065 \pm 0.081\,R_\oplus$ (without perturbations from asteroids, model E) or $6.064 \pm 0.095\,R_\oplus$ (including perturbations from the four largest asteroids, model E′). Both values are in excellent agreement with the results obtained by Giorgini et al. (2008).

We carefully examined the Apophis impact possibilities with the Earth after 2029 for VAs that will pass near the Earth at a distance between $5.6\,R_\oplus$ and $6.6\,R_\oplus$ on 2029 April 13. We showed

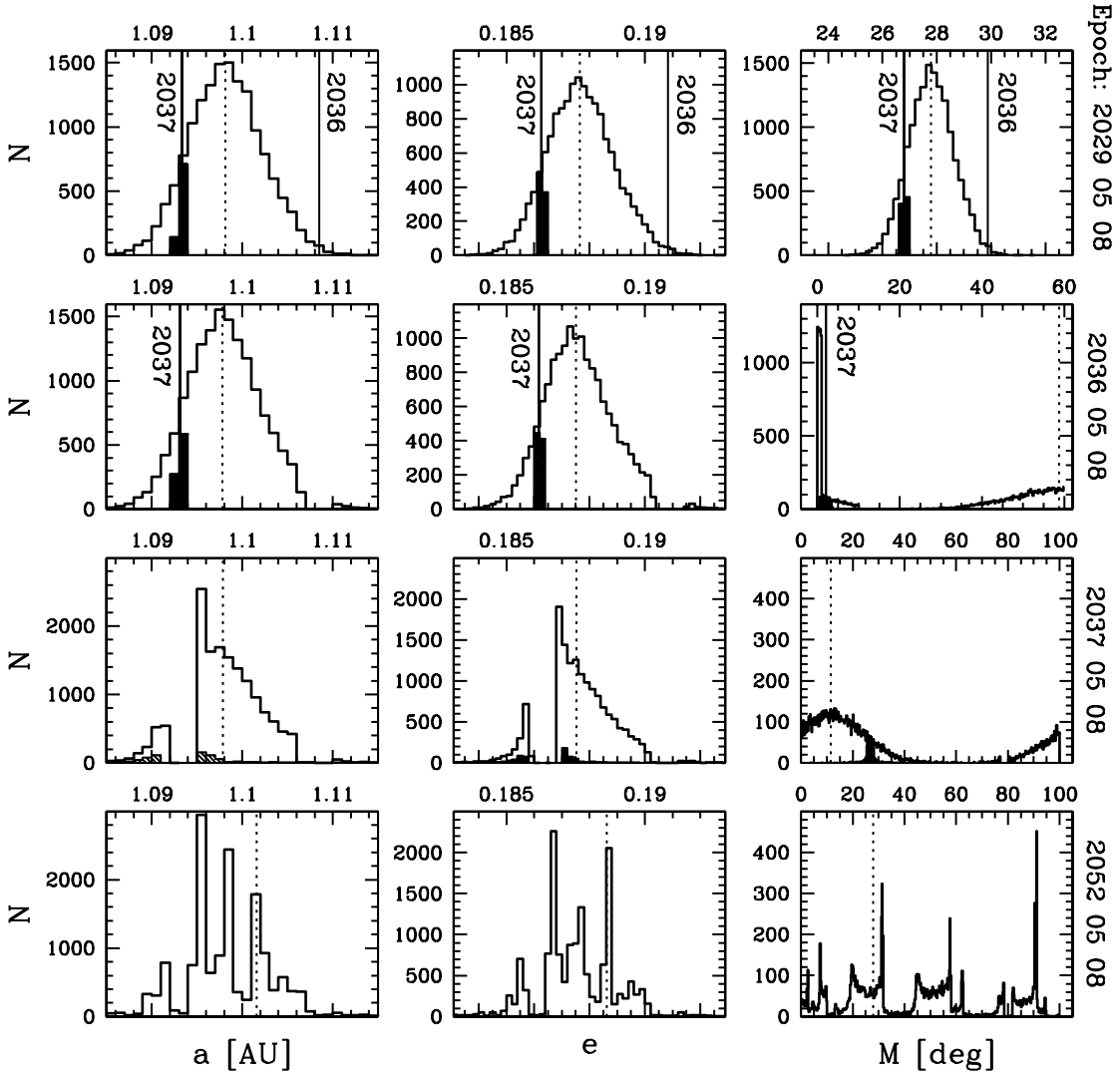

Figure 8. Evolution of potentially possible osculating orbits of Apophis obtained for model A. The starting sample of 15 000 virtual orbits was taken at the epoch of 2006 09 22. Time runs from top to bottom, and the epoch of the displayed distributions is given at the right-hand side of each row. The top row represents the distributions of a, e and M about one month after a very close encounter with the Earth in 2029 April. The position of the evolved nominal orbit is shown by the dashed vertical line. Distributions of VAs that pass closer than 0.04 au in 2037 April are denoted by filled histograms. Four impact orbits derived from this sample are given as black vertical lines (three impact orbits on 2036 April 13 and one impact orbit on 2037 April 13).

that the impact keyholes in 2036 and 2037 (or group of impact keyholes connected with the close encounter with the Earth in 2036 and 2037) are on opposite wings of the normal distribution of the minimal distance in 2029.

Our calculations provide different sizes of keyholes from those available in the literature, owing to different definitions of keyhole size and because our impact analysis is based on VAs that fill the entire volume of six-dimensional space, whereas the other impact results are limited – as far as we know – to the LOV in the parameter space. We show explicitly that some of the potential impact orbits do not lie on the LOV.

The two keyholes (or two keyhole groups) listed in Table 4 are separated by about 0.56 $R_\oplus$. Our best models E/E′ are placed almost exactly in the middle of these impact keyholes. This geometry is very fortuitous from the point of view of the impact risk, assuming that no other impact keyhole exists within this region. Unfortunately, between them we detected a narrow impact keyhole for the collision in 2076. This keyhole is situated extremely close to the nominal orbit determined by Giorgini et al. (2008) – it is separated by only about 0.01 $R_\oplus$ from their nominal value, whereas the nominal orbits derived in model E/E′ differ by about 0.09 $R_\oplus$ ($\sim$ one sigma) from the impact keyhole for the 2076 collision. The Giorgini et al. (2008) value is separated by 0.19 $R_\oplus$ ($\sim$ two sigma) and 0.38 $R_\oplus$ ($\sim$ three sigma) from the impact keyholes in 2036 and 2037, respectively. It will be important to take all of these detected keyholes into consideration during the planned mission of the *Foresight* spacecraft or any other mission to Apophis.

It should be noted that the results presented in this paper have been obtained using the independent methods of data processing, numerical orbit integration (which incorporates the non-linear terms) and generation of the VAs in the six-dimensional parameter space by means of the Monte Carlo method. It is thus encouraging that all of the common points of our results and those available in the literature are in very good agreement.

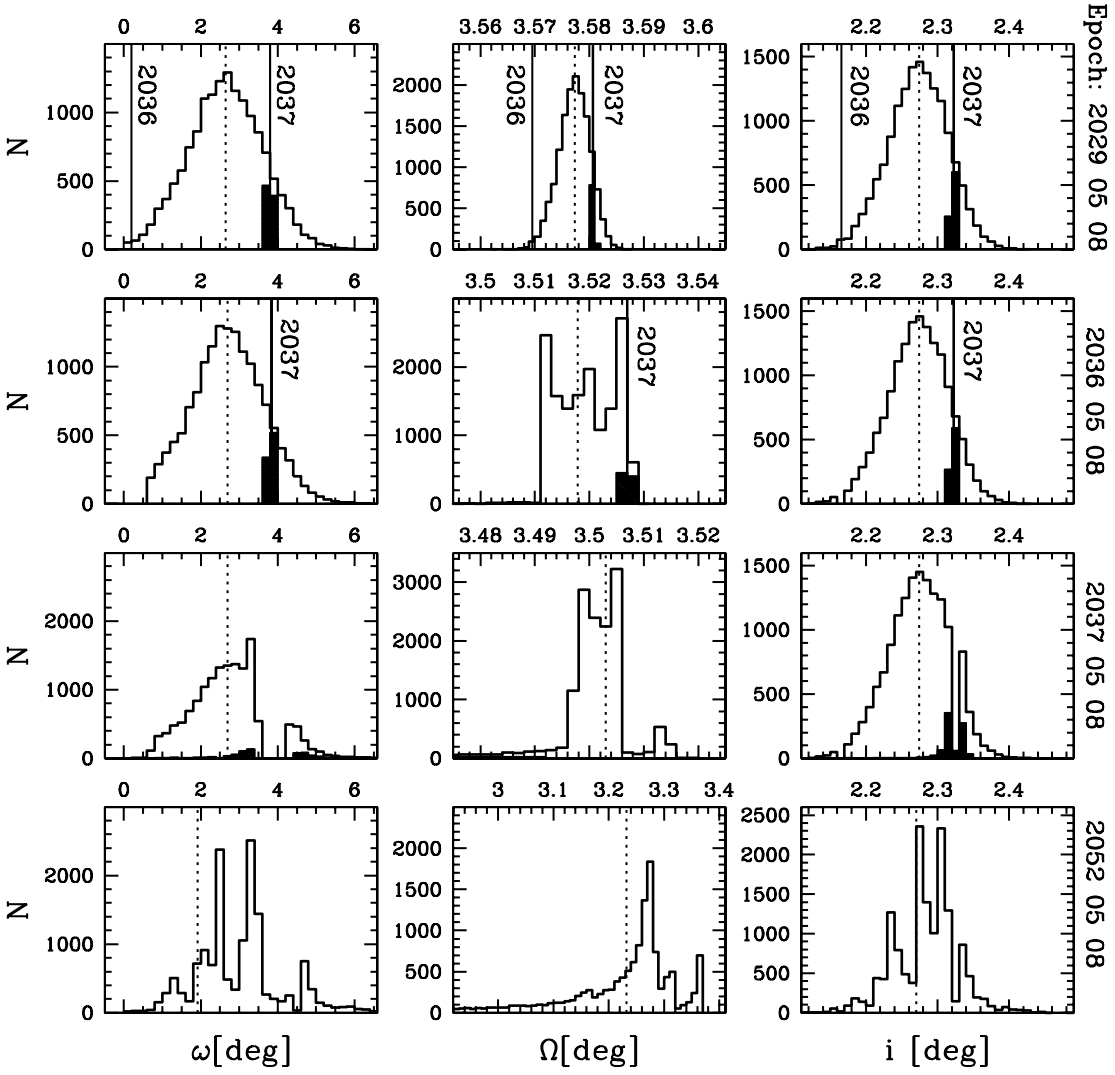

Figure 9. As Fig. 8, for ω, Ω and orbital inclination i.

ACKNOWLEDGMENTS

This work was partly supported by the Polish Committee for Scientific Research (KBN grant 4 T12E 039 28).

REFERENCES

Avni Y., 1976, ApJ, 210, 642
Bielicki M., 1972, in Chebotarev G. A., Kazimirchak-Polonskaia E. I., Marsden B. G., eds, Proc. IAU Symp. 45, The Motion, Evolution of Orbits, and Origin of Comets. Reidel, Dordrecht, p. 112
Bielicki M., Sitarski G., 1991, Acta Astron., 41, 309
Carpino M., Milani A., Chesley S. R., 2003, Icarus, 166, 248
Chauvenet W., 1908, Manual of Spherical and Practical Astronomy, Embracing the General Problems of Spherical Astronomy, the Special Applications to Nautical Astronomy, 5th edn, Vols 1–2. J.B. Lippincott, New York.
Chesley S. R., 2006, in Daniela L., Sylvio Ferraz M., Angel F. J., eds, Proc. IAU Symp. 229, Asteroids, Comets, Meteors. Kluwer, Dordrecht, p. 215
Chodas P. W., 1999, BAAS, 31, 1117.
Delbò M., Cellino A., Tedesco E. F., 2007, Icarus, 188, 266
Giorgini J. D., Benner L. A. M., Nolan M. C., Ostro S. J., 2005, BAAS, 37, 636
Giorgini J. D., Benner L. A. M., Ostro S. J., Nolan M. C., Busch M. W., 2008, Icarus, 193, 1
Sansaturio M. E., Arratia O., 2008, Earth Moon Planets, 102, 425
Sitarski G., 1979, Acta Astron., 29, 413
Sitarski G., 1989, Acta Astron., 39, 345
Sitarski G., 1998, Acta Astron., 48, 547
Sitarski G., 2002, Acta Astron., 52, 471
Sitarski G., 2006, Acta Astron., 56, 283
Smalley K. E., Garradd G. J., Benner L. A. M., Nolan M. C., Giorgini J. D., Chesley S. R., Ostro S. J., Scheeres D. J., 2005, IAU Circ., 8477, 1
Valsecchi G. B., Milani A., Gronchi G. F., Chesley S. R., 2003, A&A, 408, 1179
Vinogradova T. A., Kochetova O. M., Chernetenko Y. A., Shor V. A., Yagudina E. I., 2008, Solar System Res., 42, 271

APPENDIX A: APOPHIS ORBITAL ELEMENTS

Table A1. Comparison of orbital elements between our models E, C and the JPL Small-Body Database Browser (http://ssd.jpl.nasa.gov/) at the epoch 2009 06 18.

a	e	i	Ω	ω	M
		Model E			
0.922438326668	0.191204301641	3.331421757	204.442615749	126.404099133	117.468316749
$\mp$0.000000023128	$\mp$0.000000082841	$\mp$0.000001356	$\mp$0.000032639	$\mp$0.000032935	$\mp$0.000066920
		Model C			
0.922438293954	0.191204390446	3.331421135	204.442638994	126.404078364	117.468403784
$\mp$0.000000029556	$\mp$0.000000108748	$\mp$0.000001705	$\mp$0.000033682	$\mp$0.000034553	$\mp$0.000085400
		JPL Small-Body Database Browser			
0.922438242097	0.191204309568	3.331420536	204.442505911	126.404227544	117.468358058
$\mp$0.000000023613	$\mp$0.000000076074	$\mp$0.000002024	$\mp$0.000107210	$\mp$0.000106320	$\mp$0.000065427
Δ a/$\sigma_{\rm a}$	Δ e/$\sigma_{\rm e}$	Δ i/$\sigma_{\rm i}$	$\Delta\ \Omega/\sigma_\Omega$	$\Delta\omega/\sigma_\omega$	Δ M/$\sigma_{\rm M}$
		JPL versus model E			
2.56	0.0705	0.501	0.980	1.15	0.441
		JPL versus model C			
1.37	0.609	0.226	1.18	1.33	0.425

This paper has been typeset from a TEX/LATEX file prepared by the author.